Chinese Chemical Letters 32 (2021) 2529–2533

Contents lists available at ScienceDirect

Chinese Chemical Letters

journal homepage: www.elsevier.com/locate/cclet

Communication

Fabrication of bimetallic nanoparticles modified hollow nanoporous carbons derived from covalent organic framework for efficient degradation of 2,4-dichlorophenol

Yanshu Zhang, Gongke Li*, Yufei Hu*

School of Chemistry, Sun Yat-sen University, Guangzhou 510275, China

ARTICLE INFO

Article history:
Received 11 September 2020
Received in revised form 6 December 2020
Accepted 19 January 2021
Available online 27 January 2021

Keywords:
Covalent organic framework
Hollow structure
N-doped carbon
Bimetallic nanoparticles
2,4-Dichlorophenol
Degradation

ABSTRACT

Bimetallic nanoparticles modified hollow-structured nanoporous carbons (NPCs) have been fabricated *via* a convenient one-step carbonizing strategy derived from covalent organic framework. The Pd/Fe/NPCs, Pt/Fe/NPCs and Rh/Fe/NPCs were obtained and can be used as Fenton-like catalysts with good stability and reusability. The catalytic activity was evaluated by the degradation of 2,4-dichlorophenl (2,4-DCP). These fabricated bimetallic catalysts exhibited much higher catalytic activity than Fe/NPCs at room temperature. The enhancement of catalytic ability was benefited from synergetic catalytic effect of bimetallic nanoparticles and accelerated mass transfer of hollow structure. Additionally, the enhanced catalytic mechanism of bimetallic catalysts was studied in detail and the reasonable reaction pathway was proposed. Besides, the bimetallic catalysts were successfully used for degradation of 2,4-DCP in actual industrial wastewater and the removal efficiency could reach 74.3% within 120 min, which demonstrated the promising potential application of bimetallic catalysts in the removal of pollutants in environment.

In recent years, bimetallic nanoparticles (NPs) have attracted great attention on environmental catalysis, owing to their synergetic effects and rich active sites for enhanced catalytic performance for pollutants treatment [1,2]. Especially, iron-based bimetallic NPs have been reported as highly efficient Fenton-like catalysts for pollutants treatment due to the synergy between Fenton-like catalytic activity of Fe species and catalytic ability of other metal NPs [3]. However, the wide application of bimetallic NPs was limited by some drawbacks such as easy to aggregate or passivation and strict synthesis condition. To stabilize metal NPs on support materials is an efficient strategy to avoid metal NPs aggregation or leaching to maintain high catalytic ability. Carbon-based nanomaterials, such as porous carbon [4], grapheme oxide [5] and carbon nanotubes [6] have been regarded as suitable green supports materials because of their excellent physical and chemical properties including good stability, high specific surface area and excellent adsorption capability of pollutants [7]. However, it always needs complex functionalized process before metal NPs modification.

Recently, solid-state pyrolysis of porous organic polymers, such as metal-organic frameworks [8] and covalent organic frameworks [9,10] (COFs), have been considered as a convenient approach to fabricate carbon nanomaterials *via* carbonizing method. The nitrogen-doped carbon materials can be achieved with this method, which can offer novel physicochemical properties for various application [11]. Because of the rich nitrogen atoms can serve as coordinate sites for metal ions [12], N-doped carbon materials have been developed as new type of support materials for metal nanoparticles stabilization. Because the rich nitrogen atoms can serve as coordinate sites for metal ions, metal NPs can be stabilized on N-contained carbon materials conveniently *via* one-step combustion method in the presence of carbon sources and metal salts [13,14]. Additionally, the strong interaction between metal NPs and COFs can avoid aggregation or leaching of metal NPs and confinement effect of COFs can control the metal NPs generation and dispersion [15]. The carbon-based composites with various shapes and modified with different metal NPs can be fabricated with remarkable properties for various application [16].

COF-LZU1, which possess uniform layered organic skeleton and rich nitrogen atoms in adjacent lays, has been proved to be a suitable template for preparation of N-doped nanoporous carbon with hollow structure [17,18]. It has been indicated that hollow-structured carbon materials appear to enhance catalytic

* Corresponding authors.
E-mail addresses: cesgkl@mail.sysu.edu.cn (G. Li), huyufei@mail.sysu.edu.cn (Y. Hu).

https://doi.org/10.1016/j.cclet.2021.01.031
1001-8417/

performance because of the excellent adsorption capability [19], short mass transfer distance and low transport resistance in hollow structure [20]. In addition, the nanoporous carbons derived from COF can possess high specific surface area and porous hollow structure [21], which can facilitate bimetallic nanoparticles uniformly distribution and provide abundant catalytic active sites. Thus, noble metal NPs modified hollow-structured carbon materials derived from COFs would perform improved catalytic capability.

It is well known that, Fenton-like catalysts, such as Fe_3O_4 NPs [22,23] and nanoscale zero-valent iron systems [24], have been widely used for environmental pollutants treatment because of the strong generation of high oxidation species [25], and its potential capability to degrade organic pollutants into low toxic compounds [26]. Since the iron/noble bimetallic nanocomposite have been proved to show higher removal efficiency for pollutants due to the synergy between Fenton-like catalytic activity and hydrodechlorination catalytic ability of noble metal NPs [27,28]. Thus, co-existed iron and noble metal NPs is an ideal strategy to constitute bimetallic catalysts for enhancing catalytic performance. Based on these details, bimetallic NPs modified porous carbon materials can be prepared *via* a simple carbonization process, which would possess multiple advantages on physical structures and synergetic catalytic effect between noble metal NPs and Fenton-like catalytic ability of Fe species.

Herein, bimetallic NPs modified hollow-structured nanoporous carbons (NPCs) derived from COF were designed and synthesized. As shown in Fig. 1a, COF-LZU1 was selected to fabricate hollow-structured NPCs and prepared referring to the work of Wang *et al.* [18]. The transmission electron microscopy (TEM) image, X-ray diffraction (XRD) pattern and Fourier transform infrared (FT-IR) spectra of COF-LZU1 confirmed that COF-LZU1 was successfully synthesized (Figs. S1 and S2 in Supporting information). The bimetallic NPs can be modified into NPCs *via* a simple carbonizing method and Pd/Fe/NPCs, Pt/Fe/NPCs, Rh/Fe/NPCs were synthesized successfully. Fe/NPCs was prepared and studied as a contrast. Taking account into 2,4-dichlorophenol (2,4-DCP) is a typical high toxic chlorophenol pollutants [29], which was frequently investigated. Catalytic ability was evaluated by using 2,4-DCP as a representative target for degradation.

The morphology and structure of materials were characterized by TEM. Fig. 1 shows the TEM images of Fe/NPCs (Fig. 1b), Pd/Fe/NPCs (Fig. 1c), Pt/Fe/NPCs (Fig. 1d) and Rh/Fe/NPCs (Fig. 1e). As can be seen clearly, Fe_3O_4 NPs in Fe/NPCs shows larger size. However, much more smaller size bimetallic NPs were highly uniform incorporated into NPCs. This because of the confinement effect of the layered structure in COFs framework prevented the growth of bimetallic NPs. These uniformly distributed bimetallic NPs can expose abundant active sites to improve catalytic performance. Additionally, uniform hollow structure was observed clearly in four catalysts, which would facilitate mass transfer [20]. The diffusion of reactants between the solution and catalysts surface can be accelerated as a result to enhance catalytic performance [30].

The crystal structure and chemical elements of materials were analyzed by XRD patterns. The four catalysts showed weak and broad peaks at around 26.0° (Fig. 2a). It was attributed to the (002) plane of carbonized carbon, which demonstrated the nanoporous carbon skeletons were achieved successfully. Diffraction peaks (2θ) of Fe^0 at 44.0° and Fe_2O_3/Fe_3O_4 at 30.1°, 35.4°, 56.8°, and 62.4° were all clearly detected [9], which confirmed that Fe_3O_4 NPs and Fe^0 species were existed in four catalysts and explained excellent magnetism. Additionally, characteristic peaks of Pd, Pt and Rh crystalline were matched well with the standard. The characteristic diffraction peaks of Pd/Fe/NPCs observed at 40.1°, 46.7°, 68.2° and 82.2° (Fig. 2a-2) were corresponding to the (111), (200), (220) and (311) planes of Pd [14], respectively. The characteristic diffraction peaks of Pt/Fe/NPCs at 40.9°, 47.2°, 67.9° and 81.7° (Fig. 2a-3) were attributed to the (111), (200), (220) and (311) planes of Pt [31], respectively. And the characteristic diffraction peaks of Rh/Fe/NPCs at 41.9°, 69.9° and 84.4° (Fig. 2a-4) were corresponding to the (111), (220) and (311) planes of Rh [32], respectively. The XRD patterns results illustrated the metal NPs were modified on NPCs successfully.

X-ray photoelectron spectroscopy (XPS) analysis was performed to confirm the composition and elements chemical state of catalysts. The results were shown in Fig. 2b, C, N, O and Fe elements were all detected in four catalysts, which further confirmed the presence of Fe species and the successful generation of nanoporous carbon. These results were also proved by FT-IR spectra (Fig. S4a in Supporting information) of four catalysts. Moreover, the presence of metal NPs in four catalysts were confirmed by high-resolution XPS spectra of Fe 2p [33] (Fig. S3a), Pd 3d [34] (Fig. S3b), Pt 4f [35] (Fig. S3c) and Rh 3d [36] (Fig. S3d) in Supporting information, respectively. The Fe 2p spectrum of Pd/Fe/NPCs in Fig. S3a-2 showed peaks around 724.4, 711.1 and 706.6 eV, which assigned to Fe $2p_{1/2}$, Fe $2p_{3/2}$ and Fe^0, respectively. Same results were obtained in Fe/NPCs (Fig. S3a-1), Pt/Fe/NPCs (Fig. S3a-3) and Rh/Fe/NPCs (Fig. S3a-4). These results indicated that both Fe species and noble metal NPs were simultaneous obtained during the carbonization and coexisted in catalysts, which were also proved by previous XRD analysis. Besides, the thermogravimetric curves (Fig. S4b in Supporting information) indicated the good stability of catalysts.

As shown in Fig. 2c, four catalysts show typical IV isotherms with hysteresis loops from $P/P_0 = 0.45$ to 1.0. These results

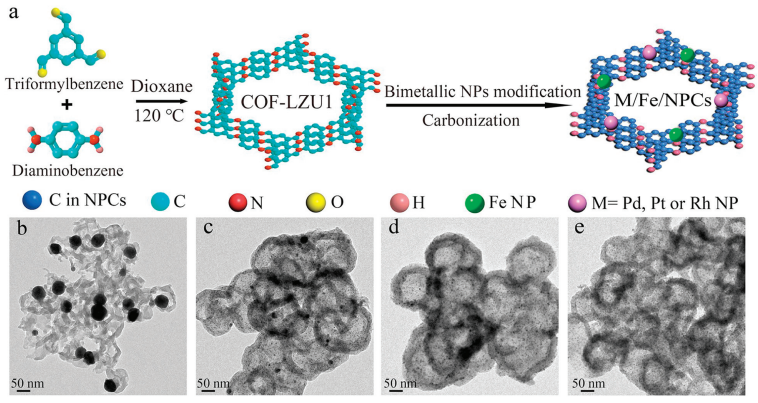

Fig. 1. (a) Schematic illustration for synthesis of bimetallic nanoparticles modified NPCs. TEM images of (b) Fe/NPCs, (c) Pd/Fe/NPCs, (d) Pt/Fe/NPCs, (e) Rh/Fe/NPCs.

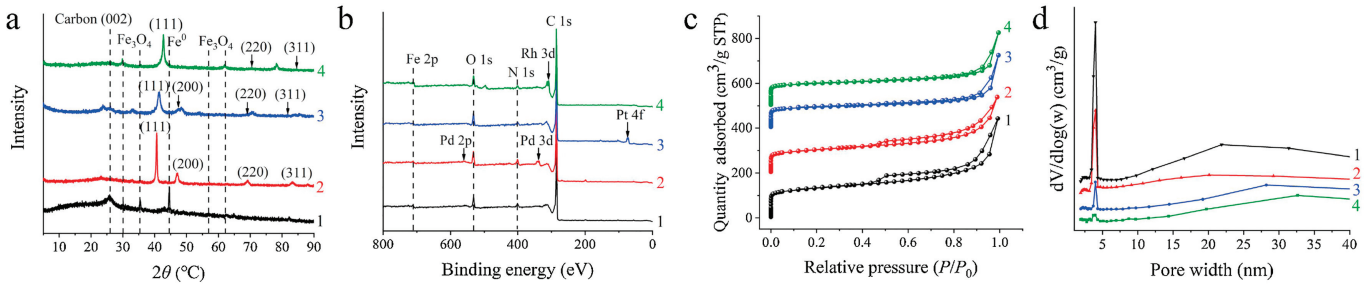

Fig. 2. Characterization of four catalysts structures: XRD patterns (a), XPS wide-scan spectra (b), N_2 adsorption and desorption isotherms (c) and the corresponding pore size distribution curves (d). The numbers 1-4 represent Fe/NPCs (1), Pd/Fe/NPCs (2), Pt/Fe/NPCs (3) and Rh/Fe/NPCs (4).

confirmed that all the catalysts have mesoporous structure [15]. The corresponding pore size distribution curves in Fig. 2d showed that the catalysts display the distribution of mesopores centered at 3.9 nm. The surface specific area of Fe/NPCs, Pd/Fe/NPCs, Pt/Fe/NPCs and Rh/Fe/NPCs calculated through the Brunauer-Emmett-Teller (BET) were 492.17, 377.05, 361.36, and 382.63 m^2/g. All the catalysts exhibited relatively high specific surface area and mesoporous structure, which could facilitate bimetallic NPs distribution to offer abundant catalytic active sites.

As generally known, pH is one of the most influence factors in the Fenton-like catalytic process [37]. 2,4-DCP degradation performed with Pd/Fe/NPCs under different pH condition were studied and results were shown in Fig. 3a. The degradation process of 2,4-DCP was found to be pH-dependent (pH = 2.0–10.0). The maximum removal efficiency was observed as 95% ± 0.8% performed with Pd/Fe/NPCs at approximately pH 2.0−6.0. The same results were found for Pt/Fe/NPCs (Fig. S5a) and Rh/Fe/NPCs (Fig. S5b), except 80% ± 1.5% for Fe/NPCs (Fig. S5c) in Supporting information. In brief, the bimetallic catalysts show much higher degradation efficiency than Fe/NPCs. The 2,4-DCP degradation efficiency declined slightly at alkaline condition (pH 8.0–10.0). This is because that, iron hydroxide would be generated on the surface of noble metal NPs, which may form passive film and inhibit subsequent iron decomposition [3]. Moreover, 2,4-DCP was ionized and negatively charged in alkaline solution. At the same time, the surface of catalysts was also negatively charged because of the adsorbed OH^-.

In this study, weak acidic and neutral condition were more suitable for 2,4-DCP degradation. Because acidic condition could dissolve more Fe species surface to expose more reactive sites. Based on XRD and XPS analysis, Fe^0 species and Fe_3O_4 NPs were co-existed in bimetallic catalysts. Thus, corrosion of Fe and formation of hydroxyl radical ($^{\bullet}OH$) were occurred in bimetallic catalytic system. The degradation process of 2,4-DCP by using bimetallic NPs as Fenton-like catalysts can be described as follows (reactions 1–4) [4,24]:

$$Fe^0 + 2H^+ \rightarrow Fe^{2+} + H_2 \quad (1)$$

$$Fe^0 + 2H_2O \rightarrow Fe^{2+} + H_2 + 2OH^- \quad (2)$$

$$Fe^{2+} + H_2O_2 \rightarrow Fe^{3+} + OH^- + {}^{\bullet}OH \quad (3)$$

$$Fe^{3+} + H_2O_2 \rightarrow Fe^{2+} + H^+ + H_2O^{\bullet} \quad (4)$$

Since Pd NPs, Pt NPs and Rh NPs are well-known good hydrogenation catalysts. The generated H_2 would transfer to noble NPs surface and being reduced to form activated hydrogen and promote Fe^0 corrosion to generate more Fe^{2+} [38]. In weak acidic conditions, along with the increase concentration of H^+, the Fe corrosion and activated hydrogen generation would be promoted. As a result, Fe^{2+} would be released easier and quicker and thereafter play a role in promoting $^{\bullet}OH$ generation (reaction 3). In brief, bimetallic catalysts facilitate iron corrosion and $^{\bullet}OH$ generation because catalytic hydrogenolysis of noble metals and Fenton-like oxidation of Fe species occurred simultaneously. The results demonstrated the synergetic catalytic effect of bimetallic NPs on 2,4-DCP degradation. According to results above, pH 5.0 was selected as optimal condition in the following experiments.

The influencee of 2,4-DCP initial concentration on 2,4-DCP degradation were studied and reaction kinetic were described with

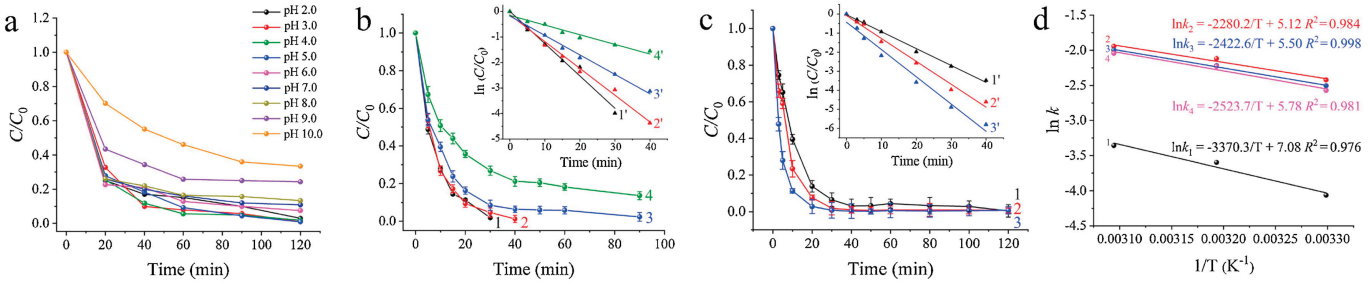

Fig. 3. (a–c): Effects of different experimental parameters on 2,4-DCP degradation performed with Pd/Fe/NPCs: (a) pH; (b) 2,4-DCP initial concentration (the numbers 1 to 4 represent 5.0, 10.0, 20.0 and 40.0 mg/L) and the inset is the fitted *pseudo*-first-order kinetics curves (1′ to 4′ represent 2,4-DCP concentration from 5.0 mg/L to 40.0 mg/L); (c) reaction temperature (the numbers 1, 2 and 3 represent reaction temperature 303 K, 313 K and 323 K) and the inset is the fitted pseudo-first-order kinetics curves (1′ to 3′ represent temperature from 303 K to 323 K). (d) Plot of ln*k* *versus* 1/T for degradation of 2,4-DCP with Fe/NPCs (line 1), Pd/Fe/NPCs (line 2), Pt/Fe/NPCs (line 3) and Rh/Fe/NPCs (line 4). Reaction conditions: pH 5.0, H_2O_2 2.0 mmol/L, catalysts dosage 0.50 g/L, 2,4-DCP 20.0 mg/L and T = 303 K.

pseudo-first-order kinetics according to Eq. S1 in Supporting information. Degradation process performed with Pd/Fe/NPCs (Fig. 3b), Fe/NPCs (Fig. S6a), Pt/Fe/NPCs (Fig. S6b) and Rh/Fe/NPCs (Fig. S6c) in Supporting information were conducted under the same condition. Along with 2,4-DCP concentration increased from 5.0 mg/L to 40.0 mg/L, 2,4-DCP removal efficiency declined and the corresponding *pseudo*-first order rate constants decreased clearly (Fig. S6 and Table S1 in Supporting information). This was because adsorption of 2,4-DCP by catalysts would reach equilibration along with the increase of 2,4-DCP concentration. In addition, high 2,4-DCP concentration would induce strong competition between reactants and intermediate products on catalytic active sits. The bimetallic catalysts showed much higher reaction rate constants than Fe/NPCs revealed higher catalytic performance. According to these results, 2,4-DCP concentration of 20.0 mg/L was selected for further study.

Investigation of catalytic kinetics under different temperatures is significant to understand reaction mechanisms. Degradation experiments at different temperatures were carried out with Pd/Fe/NPCs (Fig. 3c), Fe/NPCs (Fig. S7a), Pt/Fe/NPCs (Fig. S7b) and Rh/Fe/NPCs (Fig. S7c) in Supporting information. At 303 K, the removal efficiency was achieved 90% at 40 min with bimetallic catalysts and completely removal of 2,4-DCP was achieved within 120 min. However, 2,4-DCP can be completely removed within 40 min when temperature increased to 323 K. Along with the reaction temperature increased from 303 K to 323 K, the *pseudo*-first order rate constants of 2,4-DCP degradation also increased clearly (Table S2 in Supporting information). These results confirmed that the increase of reaction temperature facilitate catalytic process. The bimetallic catalysts showed much higher reaction rate constants than Fe/NPCs revealed the advantage of bimetallic NPs.

According to the kinetic rate constants under different temperatures, the activation energy for 2,4-DCP degradation performed with four catalysts were calculated according to Eq. S2 in Supporting information, and good liner relationships were obtained with the slope $-Ea/R$ and the intercept ln$A$ (Fig. 3d). The activation energy was calculated as follows: $E_{a(Fe/NPCs)}$ = 28.02 kJ/mol, $E_{a(Pd/Fe/NPCs)}$ = 18.96 kJ/mol, $E_{a(Pt/Fe/NPCs)}$ = 20.14 kJ/mol and $E_{a(Rh/Fe/NPCs)}$ = 20.98 kJ/mol, respectively. The bimetallic catalytic systems showed obvious lower activation energy and higher reaction rates than Fe/NPCs, which indicated that degradation process can occur more easily on bimetallic catalysts. These results were partly because of the accelerated mass transfer in hollow structure. Most importantly, hydrogenolysis process on noble NPs can facilitate iron dissolving to promote $^{\bullet}OH$ generation [39]. The degradation of 2,4-DCP with bimetallic catalysts can be performed at room temperature without any external energy, which was easy to operate and save costs greatly.

The degradation of 2,4-DCP with different catalysts dosage were also studied and results were shown in Fig. S8 in Supporting information. The bimetallic catalytic systems performed higher catalytic ability at lower catalysts dosage. The removal efficiency was achieved over 98% with 0.50 g/L catalysts dosage within 120 min. However, Fe/NPCs catalytic system need 0.75 g/L dosage to reach 95%. Considering the applicability and reducing costs, 0.50 g/L of catalysts dosage was selected as optimized condition.

In order to evaluate the stability and reusability of catalysts, recycle experiments were performed *via* magnetic recycling. Under the same conditions, degradation experiments were performed with six successive runs for Pd/Fe/NPCs, Pt/Fe/NPCs, Rh/Fe/NPCs and five runs for Fe/NPCs. The final removal efficiency in bimetallic systems was still up to 90% after six recycling process (Fig. S9 in Supporting information). The slightly decrease after three recycle runs was possible due to little loss of catalysts amount. Even for Fe/NPCs, 2,4-DCP removal efficiency was greater than 80% after 5 cycling runs. These results confirmed excellent stability and reusability of catalysts.

It is well known that Fenton-like catalytic performance is closely related to the generation of reactive oxidizing species [40]. In order to identify the reactive oxidizing species, scavenging trapping experiments were conducted by using methanol as a scavenger of $^{\bullet}OH$ [2]. Degradation of 2,4-DCP with four catalysts were all inhibited obviously after adding excess methanol (Fig. S10a in Supporting information). This indicated that $^{\bullet}OH$ was the main radical species for 2,4-DCP degradation. Electron paramagnetic resonance (EPR) spectra were studied to further confirm the generation of $^{\bullet}OH$ by using 5,5-dimethyl-1-pyrroline N-oxide (DMPO) as a spin-trapping agent [41]. As shown in Fig. S10b (Supporting information), four-fold characteristic peaks (intensity ratio of 1:2:2:1) were all observed in EPR spectra of four catalysts, which were reported as characteristic EPR signal of DMPO-$^{\bullet}OH$ spin adduct [42]. This confirmed that $^{\bullet}OH$ was generated during the degradation process. Because of the character peaks from bimetallic catalysts show stronger intensity in contrast with Fe/NPCs. Thus, the bimetallic catalytic system can generate more $^{\bullet}OH$ to enhance catalytic performance.

Furthermore, the iron dissolving (Fig. S10c in Supporting information) and H_2O_2 decomposition (Fig. S10d in Supporting information) experiments were conducted to understand the reaction mechanism. The concentration of dissolved iron increased obviously corresponding to the decomposition of H_2O_2. This result was caused by the continuous leaching of Fe^{2+}/Fe^{3+} from catalysts to solution [43]. The Fe^{2+} leached from catalysts can react with H_2O_2 to generate $^{\bullet}OH$, at the same time, Fe^{2+} was also produced continually from Fe^0. In bimetallic catalytic systems, the dissolved iron concentration increased quickly in initial 40 min, which coincide exactly with the results of rapidly increased removal efficiency within 40 min and the higher reaction rate constants. Also, the dissolved iron concentrations in bimetallic systems were fairly close and substantially higher than pure Fe/NPCs. Besides, the H_2O_2 decomposition performed with Fe/NPCs showed much slower than bimetallic catalysts (Fig. S10d). Because iron corrosion and Fe^{2+} generation occurred faster with bimetallic catalysts, as a result to promoted H_2O_2 decomposition and accelerated $^{\bullet}OH$ generation. In addition, the hollow structure can accelerate diffusion of $^{\bullet}OH$ to accelerate degradation process. These facts further confirmed the unique synergetic catalytic effect in bimetallic catalytic systems to improve catalytic performance.

In order to make an intensive study of the catalytic mechanism of bimetallic catalysts, Pd/Fe/NPCs was selected because of the higher reaction rate. The intermediates were analyzed by UPLC-MS/MS technique (Fig. S11 in Supporting information).

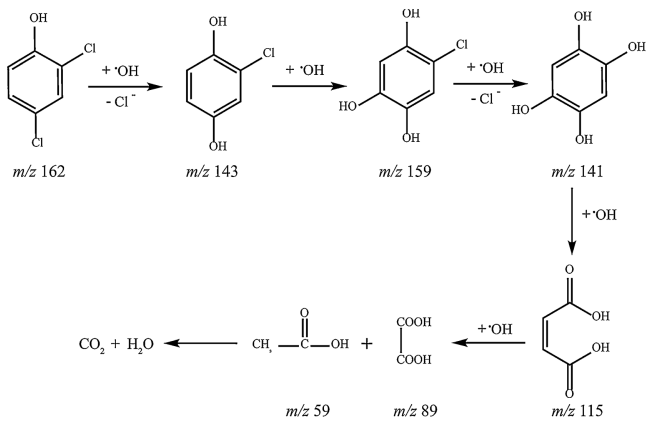

Scheme 1. Proposed reaction pathway for the degradation of 2,4-DCP performed with Pd/Fe/NPCs.

The $^{\bullet}$OH played as the main attacking reactive species for 2,4-DCP degradation and the reaction process were described in detail. Based on above results, a reasonable reaction pathway for 2,4-DCP degradation with bimetallic catalysts was proposed in Scheme 1. The degradation products were environmental-friendly, which illustrated that these bimetallic catalysts have great potential application in pollutants treatment in environment.

Subsequently, the Pd/Fe/NPCs was used as a typical bimetallic catalyst to study the feasibility of 2,4-DCP removal in actual industrial wastewater. The removal efficiency of 2,4-DCP in pharmaceutical wastewater sample within 120 min was 74.3% (Fig. S12 in Supporting information). This result indicated the good performance of bimetallic catalysts for the removal organic pollutants in wastewater. Thus, bimetallic catalysts have great potential for application in environmental wastewater treatment.

In summary, we offer an effective strategy for fabrication of bimetallic NPs modified Fenton-like catalysts with hollow structure derived from N-contained COF-LZU1 *via* a convenient one-step carbonizing method. The catalytic activity can be improved based on two aspects: One the one hand, the hollow porous structure could accelerate mass transfer and high surface areas would be beneficial to homogeneous distribution of bimetallic NPs to provide abundant catalytic active sites. On the other hand, bimetallic catalysts showed significantly synergetic catalytic effect to facilitate iron corrosion and $^{\bullet}$OH generation to enhance Fenton-like performance. The highly toxic 2,4-DCP was used as a represent to evaluate catalytic activity and the removal efficiency can reach 90% within 40 min. The bimetallic catalysts showed obviously enhanced catalytic activity compared with Fe/NPCs at room temperature without complex instrumentation. Moreover, the good recyclability of bimetallic catalysts was proved by magnetic separation experiments. Besides, the catalytic mechanism of bimetallic catalysts was studied in detail. Finally, the bimetallic catalysts were used for the degradation of 2,4-DCP in actual industrial wastewater, which revealed the great potential for application in pollutants treatment in environment. The COF template can be expended to other N-contained organic polymers for metal NPs modification or other porous structures with excellent mass transfer. Additionally, the bimetallic NPs modified carbon-based materials are expected to be applied in various catalytic application when replaced by other bimetallic NPs.

Declaration of competing interest

The authors declare that they have no known competing financial interests or personal relationships that could have appeared to influence the work reported in this paper.

Acknowledgments

This work was supported by the National Natural Science Foundation of China (Nos. 21675178, 21775167 and 21976213), the National Key Research and Development Program of China (No. 2019YFC1606101), and the Research and Development Plan for Key Areas of Food Safety in Guangdong Province of China (No. 2019B020211001), respectively.

Appendix A. Supplementary data

Supplementary material related to this article can be found, in the online version, at doi:https://doi.org/10.1016/j.cclet.2021.01.031.

References

[1] J.J. Wei, X.H. Xu, Y. Liu, D.H. Wang, Water Res. 40 (2006) 348–354.
[2] H. Zhang, Q.Q. Ji, L.D. Lai, G. Yao, B. Lai, Chin. Chem. Lett. 30 (2019) 1129–1132.
[3] J. Xu, L.S. Tan, S.A. Baig, et al., Chem. Eng. J. 231 (2013) 26–35.
[4] Y.Y. Zhou, L. Tang, G.D. Yang, et al., Catal. Sci. Technol. 6 (2016) 1930–1939.
[5] X.J. Chen, Y.Z. Dai, X.Y. Wang, et al., J. Hazard. Mater. 292 (2015) 9–18.
[6] J. Xu, X.S. Lv, J.D. Li, et al., J. Hazard. Mater. 225-226 (2012) 36–45.
[7] R. Yang, Y. Lin, B.Y. Liu, et al., Anal. Chem. 92 (2020) 3528–3534.
[8] R.M. Frizzarin, C.P. Cabello, M.M. Bauza, et al., Anal. Chem. 88 (2016) 6990–6995.
[9] X.J. Zhang, G. Zhu, M. Wang, et al., Carbon 116 (2017) 686–694.
[10] X.J. Zhao, P. Pachfule, S. Li, et al., Chem. Mater. 31 (2019) 3274–3280.
[11] X.W. Hu, Y. Long, M.Y. Fan, et al., Appl. Catal. B: Environ. 244 (2019) 25–35.
[12] Z.L. Du, Q.Q. Dang, X.M. Zhang, Ind. Eng. Chem. Res. 56 (2017) 4275–4280.
[13] X.F. Han, J. Chen, Z. Li, H.D. Qiu, Anal. Chim. Acta 1078 (2019) 78–89.
[14] X.X. Yang, Y.J. He, L.Y. Li, et al., Chem. Eur. J. 26 (2020) 1864–1870.
[15] M.Y. Fan, Y. Long, Y.Y. Zhu, X.W. Hu, Z.P. Dong, Appl. Cata. A: Gen. 568 (2018) 130–138.
[16] L.J. Song, H.J. Zhang, T.P. Cai, et al., Chin. Chem. Lett. 30 (2019) 863–866.
[17] L.Y. Chen, L. Zhang, Z.J. Chen, et al., Chem. Sci. 7 (2016) 6015–6020.
[18] S.Y. Ding, J. Gao, Q. Wang, et al., J. Am. Chem. Soc. 133 (2011) 19816–19822.
[19] X.B. Wang, Y.L. Qin, L.H. Zhu, H.Q. Tang, Environ. Sci. Technol. 49 (2015) 6855–6864.
[20] Y.M. Zhang, F. Wang, P. Ou, et al., J. Hazard. Mater. 360 (2018) 223–232.
[21] Z.Y. Lu, Z.X. Shi, S.M. Huang, et al., Talanta 214 (2020) 120864.
[22] X.Y. Yang, X.W. Cheng, A.A. Elzatahry, et al., Chin. Chem. Lett. 30 (2019) 324–330.
[23] L.J. Xu, J.L. Wang, Appl. Catal. B: Environ. 123-124 (2012) 117–126.
[24] R.C. Li, Y. Gao, X.Y. Jin, et al., J. Colloid Interface Sci. 438 (2015) 87–93.
[25] K. Chen, G.H. Wang, W.B. Li, et al., Chin. Chem. Lett. 25 (2014) 1455–1460.
[26] B. Shen, C.C. Dong, J.H. Ji, M.Y. Xing, J.L. Zhang, Chin. Chem. Lett. 30 (2019) 2205–2210.
[27] J. Xu, J. Tang, S.A. Baig, X.S. Lv, X.H. Xu, J. Hazard. Mater. 244 (2013) 628–636.
[28] D.M. Zhao, Y.Y. Zheng, M. Li, et al., Ultrason. Sonochem. 21 (2014) 1714–1721.
[29] L. Liu, W.K. Meng, L. Li, et al., Chem. Eng. J. 369 (2019) 920–927.
[30] L. Tang, Y.N. Liu, J.J. Wang, et al., Appl. Catal. B: Environ. 231 (2018) 1–10.
[31] S. Pothaya, J.R. Regalbuto, J.R. Monnier, K. Punyawudho, Int. J. Hydrogen Energy 44 (2019) 26361–26372.
[32] J.Y. Zhu, S. Chen, Q. Xue, et al., Appl. Catal. B: Environ. 264 (2020) 118520.
[33] Y.H. Zhong, Z.F. Chen, S.C. Yan, et al., Environ. Sci: Nano 6 (2019) 2986–2999.
[34] P. Zhang, R. Li, Y.M. Huang, Q.W. Chen, ACS Appl. Mater. Interfaces 6 (2014) 2671–2678.
[35] J. Liu, J.Q. Li, J.F. Rong, et al., Appl. Surf. Sci. 464 (2019) 146–152.
[36] A. Serrano-Maldonado, S.S. Rozenel, J.L. Jimenez-Santiago, I. Guerrero-Ríos, E. Martin, Catal. Sci. Technol. 8 (2018) 4373–4382.
[37] C. Zhang, M.H. Zhou, G.B. Ren, et al., Water Res. 70 (2015) 414–424.
[38] J. Xu, Z. Cao, X. Liu, et al., J. Hazard. Mater. 317 (2016) 656–666.
[39] L.P. Fang, C.H. Xu, W.B. Zhang, L.Z. Huang, Appl. Surf. Sci. 435 (2018) 55–64.
[40] L. Wan, H.Y. Song, J.H. Ma, et al., ACS Appl. Mater. Interfaces 10 (2018) 13028–13039.
[41] C.Q. Tan, Y.J. Dong, D.F. Fu, et al., Chem. Eng. J. 334 (2018) 1006–1015.
[42] M.N. Zhang, J. Jia, K. Huang, X.D. Hou, C.B. Zheng, Chin. Chem. Lett. 29 (2018) 456–460.
[43] R. Zhou, N.F. Shen, J. Zhao, Y. Su, H.J. Ren, J. Mater. Chem. A 6 (2018) 1275–1283.